

# Robustness of non-abelian holonomic quantum gates against parametric noise

Paolo Solinas,<sup>1</sup> Paolo Zanardi,<sup>2,3</sup> Nino Zanghì<sup>1</sup>

<sup>1</sup> Istituto Nazionale di Fisica Nucleare (INFN) and Dipartimento di Fisica,  
Università di Genova, Via Dodecaneso 33, 16146 Genova, Italy

<sup>2</sup> Department of Mechanical Engineering, Massachusetts Institute of Technology, Cambridge Massachusetts 02139

<sup>3</sup> Institute for Scientific Interchange (ISI), Viale Settimio Severo 65, 10133 Torino, Italy  
(Dated: December 8, 2018)

We present a numerical study of the robustness of non-abelian holonomic quantum gates. We take into account the parametric noise due to stochastic fluctuations of the control fields which drive the time-dependent Hamiltonian along an adiabatic loop. The performance estimator used is the fidelity. We carried over our analysis with different correlation times for the noise in order to understand whether there are regions in which the holonomic gates are robust. We found out that noisy holonomic gates seem to be close to the ideal ones for 'short' and 'long' noise correlation times. This result can be interpreted as a consequence of the geometric nature of the holonomic operator. A first comparison of holonomic and dynamical gates shows that there are situations in which the former are more resilient to noise than the latter ones.

PACS numbers: 03.67.Lx

## I. INTRODUCTION

The use of uniquely quantum phenomena to process information has led to surprising results in quantum key distributions [1], information transfer protocols [2] and computation [3]. From the point of view of the actual implementation of these theoretical protocols a main challenge is posed by the fact that generically quantum states are very delicate objects quite difficult to control with the required accuracy. The interaction with the many degrees of freedom of the environment causes the loss of information (decoherence) and moreover errors in processing the information lead to a wrong output state (control errors). The first problem has been extensively studied over the past few years and a few ways to overcome it have been proposed and experimentally realized. These strategies include error avoiding [4], error correcting strategies [5] and decoupling techniques [6].

A new approach called topological quantum computation has been argued to be able to effectively solve both of them and open new ways to inherently robust quantum computation [7]. Information is encoded in topological degrees of freedom of a system which are not sensitive to the local environment-noise effects and then are robust against decoherence [8]. Unfortunately to the date, no simple feasible physical system has been identified to this aim; in fact, the systems proposed are usually complicated many-particle ones living over a macroscopic non-trivial structure (e.g. torus or cylinder topology). On the other hand, we can develop topological information processing, where the operator used depends on topological controls and then are robust against the unwanted fluctuations of the driving fields. In this case, a important intermediate step is the geometrical quantum computation and particularly promising is the fully-geometrical approach called Holonomic Quantum Computation (HQC) [9].

At variance with topological information processing,

for geometrical QC several implementation proposals have been made; indeed the holonomic structure shows up in a variety of quantum systems, both in its Abelian (Berry) [10] and non-Abelian version [11, 12, 13, 14]. For this reason interest around HQC has recently grown leading also to proposals in which the adiabatic request can be relaxed and for implementing geometrical non-adiabatic quantum computation [15]. One of the apparent advantages of HQC is that the gating time for holonomic gates does not depend on the logical operator applied but only on the adiabatic request; then HQC may lead to a new approach to implement complex operators difficult to construct with the standard dynamical gates (as discussed in [14]). In view of its geometric nature i.e., dependence on areas spanned by loops in the control parameter manifold, HQC has been suggested to be robust against some class of errors [16, 17]. Nevertheless thorough studies aimed to address this important issue are still relatively few and certainly not exhaustive [18].

In this paper we will deal with the noise due to imprecise control of the system parameters during the evolution. This error source will be referred to as parametric noise. We will show that the fidelity of the holonomic gates displays three regimes, depending on the ratio between the adiabatic time and the noise correlation time. This result can be understood in view of the geometrical dependence of the holonomic operator.

In section II, after a brief review of the holonomic approach, we describe the system used and the logical gate studied; moreover, it is discussed how we model the noise in the control parameters. In Sec. III we give a description of our simulations and show the results with different kind of noise processes. A comparison with dynamical gates subject to the same noise is given too. Section IV contains the conclusions.

## II. HOLONOMIC QUANTUM GATES WITH PARAMETRIC NOISE

Let us consider a family  $F$  of isodegenerate Hamiltonians  $H(\lambda)$  depending on  $m$  dynamically controllable parameters  $\lambda$ , in the HQC approach [9] one encodes the information in a  $n$ -fold degenerate eigenspace  $E$  of an Hamiltonian  $H(\lambda_0)$ . Varying the  $\lambda$ 's and driving adiabatically  $H(\lambda)$  along a loop in the  $m$ -manifold we produce a non-trivial transformation of the initial state  $|j_0\rangle \rightarrow U|j_0\rangle$ . These transformations, known as holonomies, are the generalization of Berry's phase and can be computed in terms of the Wilczek-Zee gauge connection [19]:  $U(C) = P \exp(\oint_C A)$  where  $C$  is the loop in the parameter space and  $A = \sum_{i=1}^m A_i d\lambda_i$  is the  $u(n)$ -valued connection. If  $|\mathcal{P}_i(\lambda)\rangle$  ( $i = 1; \dots; n$ ) are the instantaneous eigenstates of  $H(\lambda)$ , the connection is  $(A)_{ij} = i\langle \mathcal{P}_i | \partial_{\lambda_j} | \mathcal{P}_i \rangle$ , ( $i, j = 1; \dots; n$ ). The set of holonomies associated with a given connection is known to be a subgroup of the group of all possible  $n$ -dimensional unitary transformations; when the dimension of this holonomy group coincides with the dimension of  $U(n)$  one is able to perform universal quantum computation with holonomies [9].

For concreteness in this paper we will focus on the HQC model analyzed in [13, 14] where the logical qubits were given by polarized excitonic states controlled by femtosecond laser pulses. We will restrict ourselves to one-qubit gates. Despite this might look at first as a major limitation, we observe that, as far as the holonomic structure is concerned, the two-qubit gates are very similar. So we expect that most of the results we are going to present here e.g., the existence of separate regimes, should, to a large extent, hold true for two-qubit gates too.

The time-dependent interaction Hamiltonian in the interaction picture is

$$H_{int} = \sum_{i=+;0} \left( \tilde{\mu}_i^+ \mathcal{P}_L^+ |i\rangle + \tilde{\mu}_i \mathcal{P}_L |i\rangle + \mu_0 \mathcal{P}_L^0 |i\rangle \right) \mathcal{H} |j\rangle + h.c. \quad (1)$$

where  $|\mathcal{P}_L^i\rangle$  ( $i = +; 0$ ) are the polarized excitonic states (two logical and one ancilla) and  $|\mathcal{P}_L^0\rangle$  is the ground state (absence of exciton). This Hamiltonian family admits two dark states i.e.,  $H_{int}(\lambda) |\mathcal{P}_i(\lambda)\rangle = 0$ ; ( $i = 1; 2$ ): This two-fold degenerate manifold represents our encoded logical qubit:  $|\mathcal{P}_L^+\rangle = |\mathcal{P}_L^+ \rangle$ ;  $|\mathcal{P}_L^-\rangle = |\mathcal{P}_L^- \rangle$ . In Ref. [12, 13] it has been shown that the Wilczek-Zee connection associated to the Hamiltonian family (1) allows to construct universal one-qubit gates. These are realized by giving an explicit prescription for driving the control parameter  $\lambda$ 's along suitable adiabatic loops.

We suppose now to add to the control field a 'small' noise which perturbs our trajectory on the control manifold. We test the robustness of the geometrical mixing single-qubit gate proposed in ref. [13]. To obtain this gate, we made the following loop in the parameter space:  $\lambda(t) = \sin \cos'$ ,  $\mu_+(t) = \sin \sin'$  and

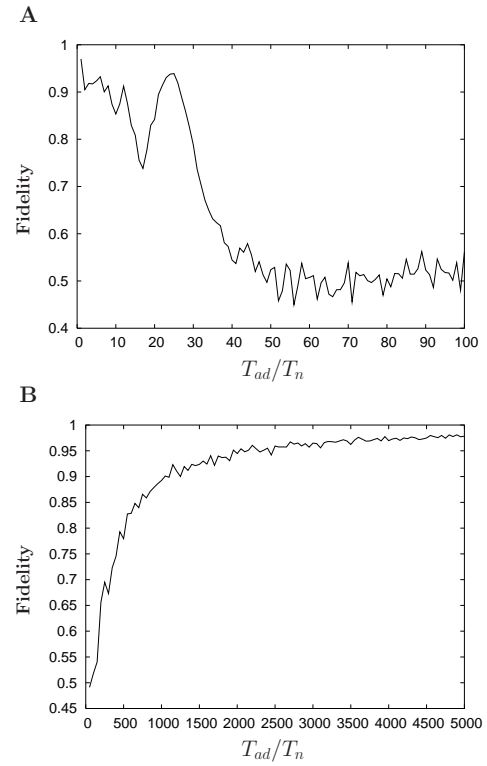


FIG. 1: Fidelity for holonomic gate with  $\tau = 50$  fs,  $T_{ad} = 7.5$  ps ( $T_{ad} = 150$ ) and  $\epsilon = 0.1$ . (A) slowly varying fluctuations and (B) slowly varying fluctuations.

$\mu_0(t) = \cos$  (where the parameters is fixed and the  $\lambda(t)$  and  $\mu'(t)$  are time dependent) and the holonomic operator obtained at the end of the loop is  $U = e^{i\gamma}$ , (where  $i\gamma = \oint_C A = \int_{\mathcal{P}_L^+}^{\mathcal{P}_L^-} i\langle \mathcal{P}_L^+ | \partial_{\lambda} | \mathcal{P}_L^+ \rangle - \int_{\mathcal{P}_L^-}^{\mathcal{P}_L^+} i\langle \mathcal{P}_L^- | \partial_{\lambda} | \mathcal{P}_L^- \rangle$ ). The geometrical parameter  $\gamma = \sin d d'$  is the solid angle spanned by the parameter vector  $\tilde{\mu} = (\mu_+; \mu_-; \mu_0)$  on the parameter manifold (sphere). Changing the relation between  $\mu_+$  and  $\mu_-$  we change the loop and then the value of  $\gamma$ . We choose a loop in order to obtain  $\gamma = \pi/2$  and  $U = \exp(i\gamma/2) = \int_{\mathcal{P}_L^+}^{\mathcal{P}_L^-} i\langle \mathcal{P}_L^+ | \partial_{\lambda} | \mathcal{P}_L^+ \rangle - \int_{\mathcal{P}_L^-}^{\mathcal{P}_L^+} i\langle \mathcal{P}_L^- | \partial_{\lambda} | \mathcal{P}_L^- \rangle$ .

The logical operator  $U$  depends only on geometrical parameters (i.e. solid angle swept on the parameters manifold), every perturbation that changes the trajectory in the control manifold changes the operator leading to computational errors. This notwithstanding, the perturbations leaving (almost) unchanged this angle will not affect the holonomic operator. Then we expect that even strong fluctuations – provided their time scale is sufficiently fast – average out, leaving in this way the angle unchanged and thus not affecting the computation.

The control parameters are the intensities and the phases of the lasers (since we suppose to be in resonant condition, we have fixed frequencies) perturbed by external noise (one for the phases and one for the intensities). To clarify which of these mainly affects the gate operation, first we separate the two types of errors (intensity and phase fluctuations) and then we apply both of them.

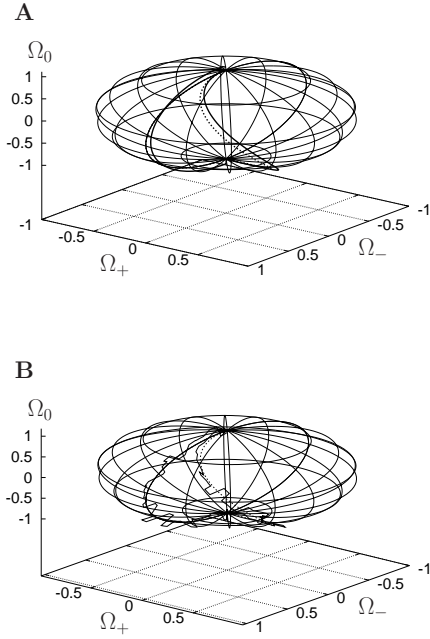


FIG. 2: Loop in the parameter space for the holonomic gate with (solid line) and without noise (dashed line). With extraction of 2 ( $T_n = T_{ad}=2$ ) (A) and 70 random numbers ( $T_n = T_{ad}=70$ ) (B). The sphere radius is normalized to  $r = 1$ .

We use a straightforward model for the noise : we extract a random number from a probability distribution, we add a constant noisy field for the time  $T_n$  to the evolving control field, then we extract another random number and so on. To simplify the simulations we choose  $T_n$  in such a way that  $T_{ad}$  is a multiple of  $T_n$  ( $T_{ad} = n_r T_n$ ). The fundamental parameter is the noise time  $T_n$  that is the lapse of time of each random extraction; i.e. it represents the time scale of each random fluctuation.

For the 'intensity' noise we modify only the value of the Rabi frequencies. We have three lasers turned on and we suppose they have independent fluctuations  $\delta \Omega_i$  (i.e. every  $T_n$  we extract three random numbers). The evolution on the control manifold is described by:

$$\begin{aligned} \dot{\langle} & (t) = \sin \cos' + \delta \Omega_0 (t) \\ & + (t) = \sin \sin' + \delta \Omega_+ (t) \\ : & 0 (t) = \cos + \delta \Omega_- (t) \end{aligned}$$

In this case, the Rabi frequencies remain real parameters, but, if we introduce a 'phase' noise ( $\delta \Omega_j = e^{i \phi_j} \Omega_j$ ), they acquire an imaginary part. The random numbers are taken as before and the evolution in the control manifold is:

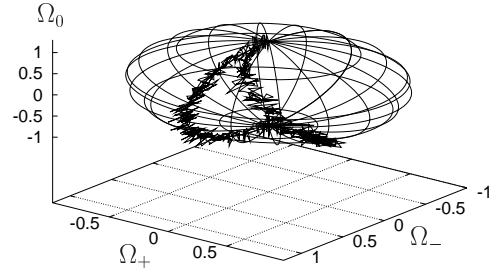


FIG. 3: Loop in the parameter space for the holonomic gate with noise and the extraction of 5000 random numbers ( $T_n = T_{ad}=5000$ ). The sphere radius is normalized to  $r = 1$ .

ifold is:

$$\begin{aligned} \dot{\langle} & (t) = e^{i \phi} \sin \cos' \\ & + (t) = e^{i \phi} \sin \sin' \\ : & 0 (t) = e^{i \phi} \cos \end{aligned}$$

The most general and complicated situation is when both 'intensity' and 'phase' noise are present.

### III. SIMULATIONS

For all the simulation we choose the parameters used in ref. [13, 14] which satisfy the adiabatic condition :  $\Omega = 0.02 \text{ fs}^{-1}$ ,  $T_{ad} = 7.5 \text{ ps}$  and  $T_{ad} = 150$ . The probability distribution for the noise is a Gaussian with zero mean and  $\langle \delta \Omega_i \delta \Omega_j \rangle = \delta_{ij}$  where  $\delta \Omega_i$  is the fluctuation of the Rabi frequency. Though this value is far below the experimental control, we use it to understand the robustness of holonomic gates against strong perturbations.

Once the evolution of the state with the noise has been computed, we must compare it with the ideal one in which the noise is absent. In order to make such a comparison quantitative we introduce the fidelity

$$F = \frac{\langle \rho_{out}^{id} | \rho_{out}^{noise} | \rho_{out}^{id} \rangle}{\langle \rho_{out}^{id} | \rho_{out}^{id} \rangle} \quad (2)$$

where  $|\rho_{out}^{id}\rangle$  is the final state without noise and  $\rho_{out}$  is the density matrix associated to the noisy final state. In our case the evolution is unitary, then  $\rho_{out} = U \rho_{in} U^\dagger$  and the fidelity reduce to be a scalar product between the noisy and the ideal state. To eliminate the dependence of (2) on the initial states we make a sampling of the initial state space and then average the results. Even if we have a four dimensional working space, we note that the initial state space has dimension

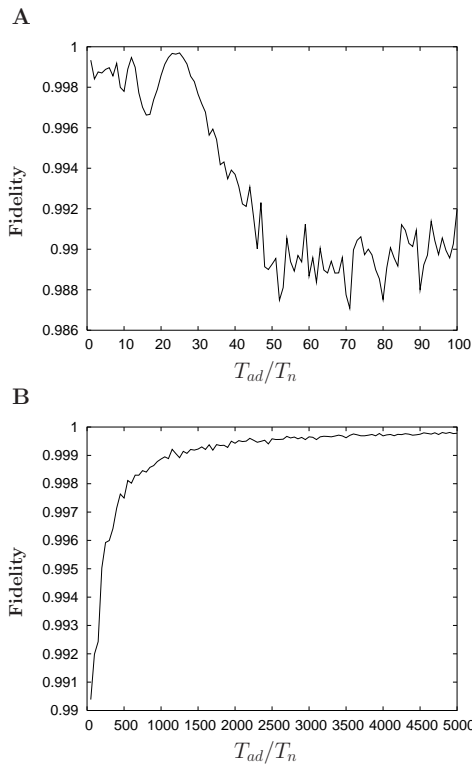


FIG. 4: Fidelity for small perturbations  $\epsilon = 0.01$ . Parameters as in figure 1.

two; in fact, in the ideal gates (once satisfied the adiabatic condition) we always start and end in a superposition of the logical states  $\mathbb{E}_L^+$  and  $\mathbb{E}_L^-$ . This simplifies the sampling procedure because we can take the Bloch sphere as sampling space. We sample the Bloch sphere with 18 states [20] and for each of them calculate the fidelity. Fixed the random numbers extracted during the evolution (i.e. fixed  $T_n$ ), we have also to take into account the dependence from the series of the random number extracted. For every sampled state we make several different realization with different extracted random numbers and calculate the average fidelity for the particular initial state. Finally, we make the average fidelity for all the sampled states to obtain the fidelity of our gate for a fixed  $T_n$ .

In the figures presented here on the y axis is plotted the fidelity and on the x axis is plotted the number of extractions (that is the the ratio  $T_{ad}=T_n$  between the adiabatic and noise time).

In figures 1 we report the simulated evolution for two regimes of noise. In figure 1 (A) we plot the fidelity when we extract up to 100 random numbers during the evolution ( $T_{ad}=100 T_n = T_{ad}$ ). Up to 30 random numbers the average fidelity is 0.875, while it decreases up to a minimum of about 0.5 (with total average of 0.632) if we extract more random numbers.

This can be better understood looking at figure 2 where we show the evolution on the parameter sphere. In figure

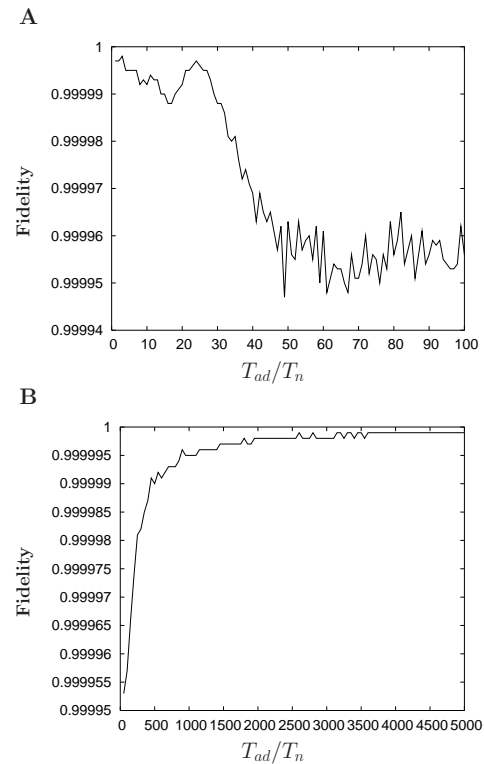


FIG. 5: Operator distance for the 'phase' noise. Parameters as in figure 1.

2 (A)  $n_r = 2$  ( $T_n = T_{ad}=2$ ) and we change the noise field twice during the evolution. Despite the intense noise, the shape of the loop is still clearly visible, it is simply shifted with respect to the ideal one. The value of the resulting solid angle swept is near to the ideal one. In figure 2 (B) we extract  $n_r = 70$  random extractions during the adiabatic evolution ( $T_n = T_{ad}=70$ ). The fluctuations are too intense and too few to cancel out then, as we expected, the solid angles, swept, respectively during the ideal and the noisy loops, are different. This can explain the result in figure 1 (A).

As stated before, even if we have strong fluctuations, we expect that if we extract many random numbers the noise in average does not affect the solid angle and leave the holonomic operator unaffected. This is what seems to be confirmed by the simulations illustrated in figure 1 (B) where we extract from 50 to 5000 random numbers. The fidelity increases and it is even better of those in figure 1 (A); the average fidelity is 0.918 but it increases to 0.956 if take into account the values from 1000 to 5000 random extractions. The relative loop in the parameter space is shown in figure (3) where we extract 5000 random numbers during the evolution: the fluctuations have  $\epsilon = 0.1$  but are so quick that cancel out.

From these simulations it is evident that we have three regimes in our model which can be explained as the sign of the geometrical dependence of the holonomic operator.:

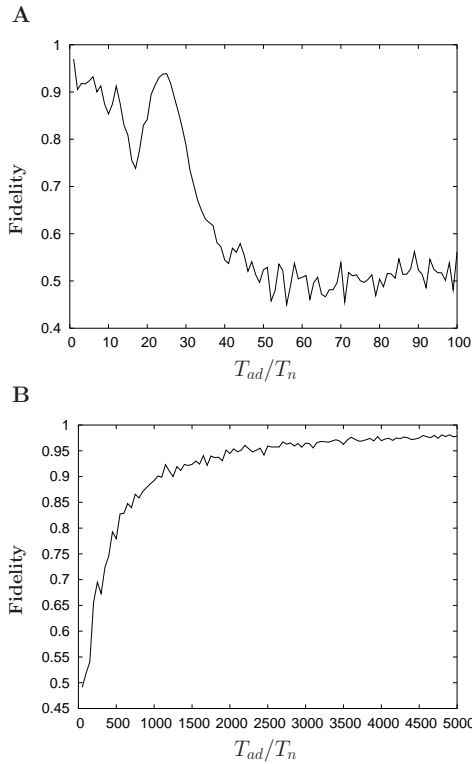


FIG. 6: Fidelity for holonomic gates when the system is subject to ‘intensity’ and ‘phase’ noise. Parameters as in figure 1.

Slowly varying random fluctuations ( $T_{ad}=T_n$ ): the loop basically maintains its shape and it is simply shifted. This situation does not affect the gate too much.

Intermediate regime ( $50 < T_{ad}=T_n < 100$ ): the intense fluctuations badly modify the loop shape and alter the gate operator.

Fastly varying random fluctuations ( $T_{ad}=T_n$ ): the fluctuations effectively cancel out and do not change the operator.

These geometrical features are independent from the ratio  $\epsilon$  and persist even for small values of the fluctuation  $\epsilon$ . If we decrease the intensity of the noise our adiabatic gate improves as shown in figures (4) where, with the same parameters (i.e. Rabi frequency and adiabatic time), we choose  $\epsilon = 0.01$ . We note that the fidelity increases but the features are the same of the previous simulations (i.e. three regimes).

In figure (5) the noise is applied only to the phase of the control field with the same adiabatic parameters of the previous simulations. Since the way of producing the operator is always the same (i.e. loop in the parameter space with a noise), we expect that the effects of noise are the same of those for ‘intensity’ noise. This can be clearly seen in figures (5) where we find the same features

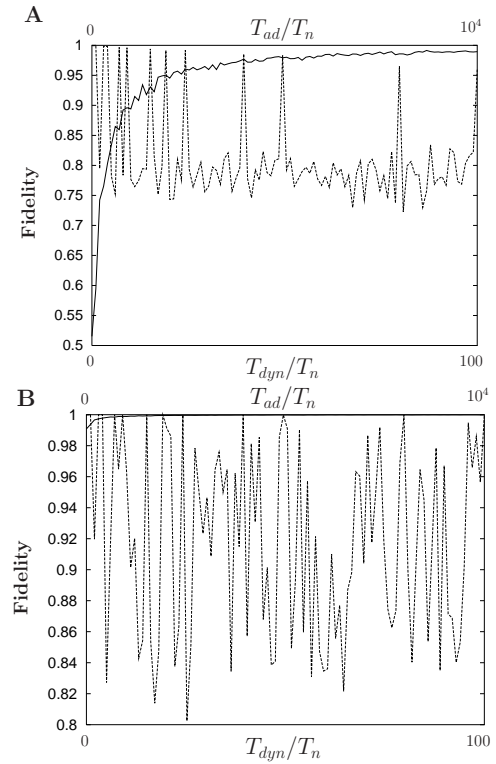


FIG. 7: Comparison between holonomic (solid line) and dynamical (dashed line) gates with (A)  $\epsilon = 0.1$  and (B) with  $\epsilon = 0.01$ . The solid curve is the holonomic one while the dashed is the dynamical one. On the top  $T_{ad}=T_n$  for the holonomic gate and on the bottom  $T_{dyn}=T_n$  for dynamical gates are reported.

of the previous plots. The fidelity is much better respect to ‘intensity’ noise and we can say the ‘phase’ noise does not affect our gate.

We finally discuss the case of both intensity and phase noise (figure 6). As we expect, the main part of the error is given by the intensity noise. The three regimes, discussed previously, are evident also in this case.

We wish to compare this holonomic gate with a standard dynamical gate, the latter one being characterized by the same unitary operator of the holonomic one and having different (typically shorter) gating time (the time need for the application of the gate). In our system this means to consider as logical states  $|j\rangle_i = |j\rangle_i$  and  $|E_L^j\rangle_i = |j\rangle_i$  and apply a pulse laser sequence to produce a transition  $|j\rangle_i \rightarrow |E_L^j\rangle_i$ .

We made similar simulations for dynamical gate with the same parameter ( $\epsilon = 0.02 \text{ fs}^{-1}$ ) and with the same noise. The results are showed as dashed line in figure (7). There is not dependence on  $T_n$  and there is a lack of features in the fidelity plot. This reflects the fact that the dynamical gates depends only on the intensities of the noisy fluctuations and not on the noise time  $T_n$ . There are strong fluctuation of the fidelity and the average value is 0.812 for  $\epsilon = 0.1$  (figure 7 (A)) and 0.921 for  $\epsilon =$

0:01 (figure 7 (B)).

In figure (7) we make a comparison between holonomic (solid line) and dynamical gates (dashed line) subject to the same intensity and phase noise. The comparison is not direct since the gating times are different. This means that the ratios  $T_{ad}=T_n$  and  $T_{dyn}=T_n$  are different for adiabatic and dynamical gates. To compare the effect of the gate subject to the same noisy field (i.e. with the same noise time  $T_n$ ), we have to take into account that the dynamical gates, in our model, are about 100 times faster than the adiabatic ones (see refs. [13, 14]). This means that if during the adiabatic evolution the noise changes  $n_r^{ad} = T_{ad}=T_n$  times, for the dynamical gates it changes only  $n_r^{dyn} = T_{ad}=(100 T_n)$  times (if  $n_r^{dyn} < 1$  for the dynamical noise it changes only once). In other words, if for dynamical gate we extract  $n_r^{dyn}$  random numbers during the evolution, for the holonomic gate we extract  $n_r^{ad} = 100 n_r^{dyn}$  random numbers. This means that to compare the fidelities we have to look in the fast varying fluctuating noise ( $T_{ad}=T_n = 1$ ) region of the previous figures.

For this reason in figure 7 (A) and (B) we put two different scales for the adiabatic ( $T_{ad}=T_n$ ) and dynamical ( $T_{dyn}=T_n$ ) gates and the plots have been rescaled taking into account for the different gating time.

For 'small' perturbations ( $\epsilon = 0.1$ ) and slowly varying random fluctuations (figure 7 (A)) the dynamical gates seem more robust than the holonomic ones ( $\langle F \rangle_{hol} = 0.777$ ) but this fact is strongly dependent on the region we analyze; in fact it is evident that when  $T_{ad}=T_n$  increases the holonomic gates are better ( $\langle F \rangle_{hol} = 0.9724$ ) with total average fidelity  $\langle F \rangle_{hol} = 0.938$  (against  $\langle F \rangle_{dyn} = 0.812$ ).

The situation definitely changes if we reduce the strength of the noise and use  $\epsilon = 0.01$  as shown in figure 7 (B). The fidelity of the holonomic gates is always better than the dynamical one with total average of  $\langle F \rangle_{hol} = 0.999$  (against  $\langle F \rangle_{dyn} = 0.921$ ) and it increases for great  $T_{ad}=T_n$ . The convergence to good fidelity for decreasing  $\epsilon$  seem much faster for the holonomic gate.

Both dynamical and holonomic gates can be further improved. Since the dynamical gates are not subject to adiabatic constraints, we can choose different parameters in order to minimize the effect of the noise but this affects the gating time.

For holonomic gates, given a noise with fixed correlation noise time  $T_n$ , we can try to change adiabatic time in order to modify the  $T_{ad}=T_n$  ratio. This should allow us to fall in a 'good' regime i.e. fast or slowly varying fluctuations. Decreasing adiabatic time to get in the small  $T_{ad}=T_n$  region can produce new errors due to the lack of adiabaticity during the evolution and then it must be treated carefully. Increasing the adiabatic time to enter in

the region of great  $T_{ad}=T_n$  leads both to a better precision in the adiabatic gates and to the cancellation of noisy fluctuations but gives longer gating times.

#### IV. CONCLUSIONS

We numerically studied the robustness of a non-abelian holonomic quantum gate against stochastic errors in control parameters. The robustness of logical gates show three regimes upon the variations of the noise correlation time  $T_n$ . These regimes can be understood on the basis of the geometric (i.e. solid angle swept in the parameter space) dependence of the holonomic operator. For fast random varying fluctuations we have a good robustness of the holonomic gate since, as argued in other papers [16, 17], the fluctuations during the loop tend to cancel out. For random varying fluctuations in the intermediate regime the holonomic gates are significantly corrupted because the fluctuations strongly deform the parameter loop. For slowly random varying fluctuations the performance improves again. This fact is not surprising as it may seem, indeed the loop in the parameter space turns out in this case to be simply shifted rather than deformed; then similar solid angles are swept. Our analysis suggests that the main noise source is given by fluctuations in the intensity of the control parameters whereas the phase fluctuations do not seem to sizeably affect the gate studied. The effect of the noise decreases with the variance of the intensity of the fluctuations and for  $\epsilon = 0.01$  we have medium fidelity close to 1.

A first comparison of adiabatic and dynamical gates shows that in the extreme regimes (fastly and slowly varying fluctuations) the former are more resilient to parametric noise than the latter. There is just a small window in which the dynamical gate seems better but the situation is reversed for small fluctuations ( $\epsilon = 0.01$ ) where the holonomic gate is always and definitely better than the dynamical one.

We believe that our analysis and conclusions should be extended rather easily to different sort of system proposed for HQC: for example, it definitely extends to the model proposed in ref. [12] since the involved holonomic structure is isomorphic to the one here analyzed. The general features of our results should hold also more general situations, since they apparently do not rely on the detailed features of Hamiltonian (1), rather on the general structure of holonomic computations. A related, though logically distinct, issue is the robustness of HQC against environmental decoherence [21]. This is clearly an important subject to be addressed in future investigations.

P.Z. gratefully acknowledges financial support by Cambridge-MIT Institute Limited and by the European Union project TOPQIP (Contract IST-2001-39215)

[1] C.H. Bennett and G. Brassard Proceedings of IEEE International Conference on Computers, Systems and Sig-

nal Processing 175-179, IEEE, New York, 1984. C.H.

- Bennett Phys. Rev. Lett. 68 (21), 3121, 1992.
- [2] C. H. Bennett, G. Brassard, C. Crépeau, R. Jozsa, A. Peres, and W. K. Wootters Phys. Rev. Lett. 70, 1895, 1993.
- [3] P. W. Shor Proceeding of 35th Annual symposium on foundation of Computer Science. (IEEE Computer Society Press, Los Alamitos, CA, 1994). L. K. Grover Proc. 28<sup>th</sup> Annual ACM Symposium on the Theory of Computation, 212, ACM Press, New York, 1996.
- [4] P. Zanardi and M. Rasetti, Phys. Rev. Lett. 79, 3306 (1997).
- [5] P. W. Shor Phys. Rev. A 52, 2493 (1995); A. M. Steane Phys. Rev. Lett. 77, 793 (1996); E. Knill, R. Laamme, Phys. Rev. A 55, 900 (1997) and references therein.
- [6] L. Viola and S. Lloyd, Phys. Rev. A 58, 2733 (1998); L. Viola, E. Knill, and S. Lloyd Phys. Rev. Lett. 82, 2417 (1999); D. Vitali, P. Tombesi, Phys. Rev. A 65, 012305 (2002); P. Zanardi, Phys. Lett. A 258 77 (1999)
- [7] A. Kitaev, Preprint quant-ph/9707021. M. H. Freedman, A. Kitaev, W. Zhenghan, Commun. Math. Phys. 227 587 (2002).
- [8] P. Zanardi, S. Lloyd, Phys. Rev. Lett. 90, 067902 (2003)
- [9] P. Zanardi and M. Rasetti, Phys. Lett. A 264, 94 (1999). J. Pachos, P. Zanardi and M. Rasetti, Phys. Rev. A 61, 010305(R) (2000).
- [10] J. A. Jones et al., Nature 403, 869 (2000). G. Falci et al., Nature 407, 355 (2000).
- [11] R. G. Unanyan, B. W. Shore and K. Bergmann, Phys. Rev. A 59, 2910 (1999). L. Faoro, J. Siewert and R. Fazio, Phys. Rev. Lett. 90, 028301 (2003). I. Fuentes-Guridi et al. Phys. Rev. A 66, 022102 (2002). A. Recati et al. Phys. Rev. A 66, 032309 (2002).
- [12] L.-M. Duan, J. I. Cirac and P. Zoller, Science 292, 1695 (2001).
- [13] P. Solinas et al. Phys. Rev. B 67, 121307 (2003)
- [14] P. Solinas et al. Phys. Rev. A 67, 062315 (2003)
- [15] Wang Xiang-Bin, M. Keiji Phys. Rev. Lett. 87, 097901 (2001); Wang Xiang-Bin, M. Keiji Phys. Rev. Lett. 88, 179901(E) (2002). X.-Q. Li et al. Phys. Rev. A 66, 042320 (2002). S. L. Zhu, Z. D. Wang, Phys. Rev. Lett. 89, 097902 (2002). P. Solinas et al. Phys. Rev. A 67, 052309 (2003)
- [16] J. Preskill in Introduction to Quantum Computation and Information, edited by H.-K. Lo, S. Popescu, and T. Spiller (World Scientific, Singapore, 1999).
- [17] D. Ellinas and J. Pachos, Phys. Rev. A 64, 022310 (2001).
- [18] A. B. Lais and A.-M. S. Tremblay Phys. Rev. A 67, 012308 (2003); A. Nazir, T. P. Spiller, and W. J. Munro, Phys. Rev. A 65, 042303 (2002); G. De Chiara, G. M. Palma, Phys. Rev. Lett. 91, 090404 (2003); A. Carollo et al., Phys. Rev. Lett. 90, 160402 (2003); A. Carollo et al. quant-ph/0306178; V. I. Kuvshinov, A. V. Kuzmín, Phys. Lett. A, 316, 391 (2003); F. Gaitan, quant-ph/0312008
- [19] F. Wilczek, A. Zee, Phys. Rev. Lett. 52, 2111 (1984).
- [20] Our sampling set of the Bloch sphere is given by  $\{e_{\vec{p}}\}_{\vec{p}=(x,y,z)}$ ;  $(e_x, e_y) = \frac{1}{\sqrt{2}}$ ;  $(e_x, e_z) = \frac{1}{\sqrt{2}}$ ;  $(e_y, e_z) = \frac{1}{\sqrt{2}}$ . Here  $e_i$  denotes the normalized vector of the  $i$ -th direction.
- [21] I. Fuentes-Guridi, F. Girelli, E. R. Livine, quant-ph/0311164